The effect of grain refinement on the deformation and cracking resistance in Zn–Al–Mg coatings

Ahmadi, Masoud; Salgın, Bekir; Kooi, Bart J.; Pei, Yutao

Published in:
Materials Science and Engineering A

DOI:
10.1016/j.msea.2022.142995

Publication date:
2022

Materials Science & Engineering A 840 (2022) 142995

Contents lists available at ScienceDirect

Materials Science & Engineering A

journal homepage: www.elsevier.com/locate/msea

The effect of grain refinement on the deformation and cracking resistance in Zn–Al–Mg coatings

Masoud Ahmadi [a], Bekir Salgın [b], Bart J. Kooi [c], Yutao Pei [a,*]

[a] Department of Advanced Production Engineering, Engineering and Technology Institute Groningen, Faculty of Science and Engineering, University of Groningen, Nijenborgh 4, 9747, AG, Groningen, the Netherlands
[b] Tata Steel, Research & Development, P.O. Box 10000, 1970, CA, IJmuiden, the Netherlands
[c] Nanostructured Materials and Interfaces, Zernike Institute for Advanced Materials, Faculty of Science and Engineering, University of Groningen, Nijenborgh 4, 9747, AG, Groningen, the Netherlands

ARTICLE INFO

Keywords:
Grain refinement
Cracking resistance
Zn–Al–Mg coatings
Twinning

ABSTRACT

The present study is dedicated to explore the effect of grain refinement on cracking resistance of hot-dip galvanized Zn–Al–Mg coatings on steel substrate. In this work, we demonstrate the enhancement of plastic deformation and cracking resistance by refining the microstructure (primary zinc grains) of the Zn–Al–Mg coatings. For this purpose, two types of Zn–Al–Mg coatings namely, fine grained and coarse grained microstructures are investigated utilizing *in-situ* scanning electron microscopy tensile tests. Electron backscatter diffraction technique is used to illuminate the deformation behavior at the scale of grains (and/or within grains). The results reveal that the coating with fine grained microstructure possesses higher ductility and cracking resistance, whereas the coating with coarse grain microstructure induces more transgranular cracking during deformation. Moreover, primary zinc grain refinement has been shown to decrease the fraction of coarse deformation twins that serve as undesirable sites of micro-cracking. In particular, both deformation mechanisms and cracking behavior are found to be grain size-dependent in these coatings.

1. Introduction

Zn–Al–Mg coatings offer significant anti-corrosive protection for steel substrates utilized in automotive and construction applications [1,2]. Nevertheless, the low cracking resistance of these coatings is a challenging downside which requires further improvements [3]. These coatings, typically produced by hot-dip galvanizing (HDG) process, exhibit anisotropic complex microstructures [4]. The composite structure of these coatings requires a real-time and local observation of deformation evolution at the grain level to detect the cracking sites and crack propagation. Accordingly, in order to realize a highly-formable and crack-resistant coating, process-materials design parameters need to be optimized. One of such parameters is the grain size of the coating microstructure and that is the primary motivation of the present study.

The microstructures of Zn–Al–Mg coatings with different compositions have been studied by applying various approaches before. Many studies have reported that the microstructure of these coatings is comprised of the primary Zn grains and granular/lamellar eutectic structures composed of Mg–Zn intermetallics [5–8]. The microstructures of the coatings were broadly modified using a quaternary alloying element primarily targeting anti-corrosion improvement [9,10]. It has been a continuing interest to correlate the microstructure with corrosion properties in Zn–Al–Mg coatings in the literature [11–13]. In contrast, tailoring the microstructure for the purpose of enhancing the mechanical performance and cracking resistance of these coatings lacks sufficient research work. Various studies have evaluated the mechanical response of zinc-based alloys and coatings on steel substrates [14–22]. Mechanical properties of pure zinc and Mg-alloyed zinc coatings have been reported to be affected by the weak binary eutectics (BE) within the microstructure [23], grain boundary characteristics [24,25], the steel substrates [26,27], crystallographic orientation [23,28] and texture [29,30], surface roughening, thickness and deformation mode [26,31]. In particular, the cracking behavior and formability of Zn–Al–Mg coatings on steel substrate have been scrutinized by us previously [23,24,26,29]. Based on our previous findings, the inherent properties associated with microstructural features significantly influence the resultant cracking resistance of these coatings. Grain refinement is a well-known strategy to boost the plasticity of metallic materials. This technique has been

* Corresponding author.
E-mail address: y.pei@rug.nl (Y. Pei).

https://doi.org/10.1016/j.msea.2022.142995
Received 6 December 2021; Received in revised form 8 February 2022; Accepted 14 March 2022
Available online 18 March 2022

applied in wide ranges of hexagonal close packed (HCP) alloys [32,33]. It has been shown that refining the grains can influence the deformation mechanisms by altering the dislocation slip modes and stacking fault contributions [34]. In zinc and its alloys, the microstructure mostly consists of coarse grains leading to undesired mechanical behavior. To resolve this drawback, grain refinement has been performed by addition of alloying elements or during the production and processing of the specimens [19,21,35]. In the case of hot-dip galvanized Zn–Al–Mg coatings, grain refinement has been carried out and corrosion properties have been evaluated in the literature [36]. However, the mechanical performance, specially cracking behavior of Zn–Al–Mg coatings, has not been systematically assessed as a function of grain size. In this work, by employing *in-situ* scanning electron microscopy (SEM) tensile tests and electron backscatter diffraction (EBSD) analysis, we have performed a comprehensive study of these phenomena. To achieve in-depth understanding, the deformation responses of two coatings, with fine and coarse primary zinc grain sizes within the microstructures, are explored. Particularly, we have enhanced the ductility and cracking resistance of hot-dip galvanized Zn–Al–Mg coatings by fostering grain refinement in the coating microstructure. Furthermore, we demonstrate that the deformation *mechanisms* associated with these coatings are grain size-dependent.

2. Materials and methods

In this work, an annealing hot-dip simulator was utilized to fabricate the Zn–Al–Mg coatings. ZnAlMg coating type 1 (ZC1) exhibited a fine grained microstructure and ZnAlMg coating type 2 (ZC2) had a coarse grained microstructure, both produced with the nominal composition of 1.7 wt% Al and 1.5 wt% Mg on the same interstitial free (IF) steel substrate. The microstructural refinement was accomplished by adjusting the galvanizing parameters including after-pot cooling rate and the bath temperature. The residual stresses on the samples were minimized by applying annealing during the galvanization process. The thickness of the as-produced coatings was about 15 μm, and the thickness of the steel substrate was 700 μm. The chemical composition (wt%) of the IF steel substrate used in the present study is given in Table 1.

The samples for *in-situ* tensile tests were extracted from the galvanized sheets using laser cutting with the designated dimensions provided in Fig. 1. The microstructural investigations on the tensile specimens were executed within a region (2.5 mm × 1.5 mm) at the center of the gauge (approximately 1 mm from the laser cut edges) schematically presented in Fig. 1 by a red rectangle. For the high quality characterization on all the samples in this study, a few minutes mechanical polishing utilizing 1 μm diamond suspension was first carried out on the specimens. Afterwards, ion polishing (JEOL IB-19520CCP) was employed to enhance the surface quality of the samples for microscopic characterizations.

Kammrath & Weiss tensile testing module installed in a Tescan LYRA SEM–FIB scanning electron microscope was used to perform the *in-situ* tensile tests. The SEM observation of the coating microstructures was conducted using the same microscope. Note that the *in-situ* tensile tests are performed on the total coating-substrate system. The true stress-strain curves were obtained by converting from engineering stress and strain data.

Orientation image microscopy (OIM) analysis was conducted by means of a Philips XL30 ESEM possessing an EBSD detector. In these experiments, scanning step size and applied accelerating voltage were set as 500 nm and 30 kV, respectively. All the EBSD analyses including crystallographic texture measurements were attained by using EDAX-TSL OIM™ Analysis 8 software. The characterization and testing procedures were executed at the room temperature. The grain size, phase fractions and crack area factions of the coatings were measured by meticulous image analysis performed using ImageJ software. Thresholding method was applied on SEM images to convert the features of interest (grains, phases, cracks) into binary formats, and the relevant areas were counted by image analysis to get the fraction of phases and crack area, and the average equivalent diameter of grains as the grain size.

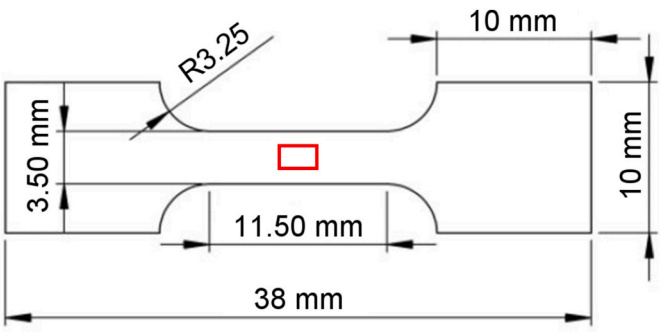

Fig. 1. The dimensions of the tensile test specimens and the region of the investigations designated by a red rectangle at the center of the gauge. (For interpretation of the references to colour in this figure legend, the reader is referred to the Web version of this article.)

3. Results and discussion

3.1. Microstructural characterization

The microstructural characteristics of ZC1 and ZC2 are revealed by SEM images given in Fig. 2. As it can be observed, ZC1's microstructure is clearly finer than that of ZC2. As indicated in Fig. 2b and d, both coatings entail three microstructural components, namely, primary zinc grains (Zn), binary eutectic (BE) and ternary eutectic (TE). The binary eutectic is composed of coarse platelets of Zn and $MgZn_2$ intermetallic compound, while ternary eutectic exhibits fine Zn, $MgZn_2$ and Al as shown in our previous work [23]. Nevertheless, the fraction of eutectic components is found to be much higher in the ZC1 coating. In particular, the fraction of BE is measured as 3% in ZC1 and 1.4% in ZC2, whereas TE constitutes 36.5% of ZC1 and 9.6% of ZC2. Therefore in total, eutectics (BE + TE) constitute 39.5% and 11% of ZC1 and ZC2, respectively. It is worth noticing that the primary zinc grains of both coatings encompass precipitates which are mostly nanometer-sized Al-rich precipitates [24]. The precipitation in primary zinc grains is identified as a significant strengthening mechanism of Zn–Al–Mg coating as shown by us [24]. Furthermore, the quantified primary zinc grain sizes associated with the coating ZC1 and ZC2 are given in Fig. 3. ZC2 microstructure possesses over five times larger grain size compared to that of ZC1. The average size of the primary zinc grains in the coating ZC1 reaches 9 μm, whereas it is found to be 56 μm in the case of ZC2. This pronounced contrast in the size of primary zinc grains enables a reasonable comparison of deformed microstructures as a function of grain size.

3.2. EBSD analysis prior to deformation

The crystallographic texture of the coatings should be studied prior to deformation in order to exclude the influence of texture on the

Table 1
The chemical composition (wt%) of the IF steel substrate used in this study.

C	Mn	Al	Ti	Ni	Cr	Cu	S	P	Si	Sn
0.02	0.65	0.57	0.47	0.22	0.17	0.14	0.06	0.04	0.04	0.03

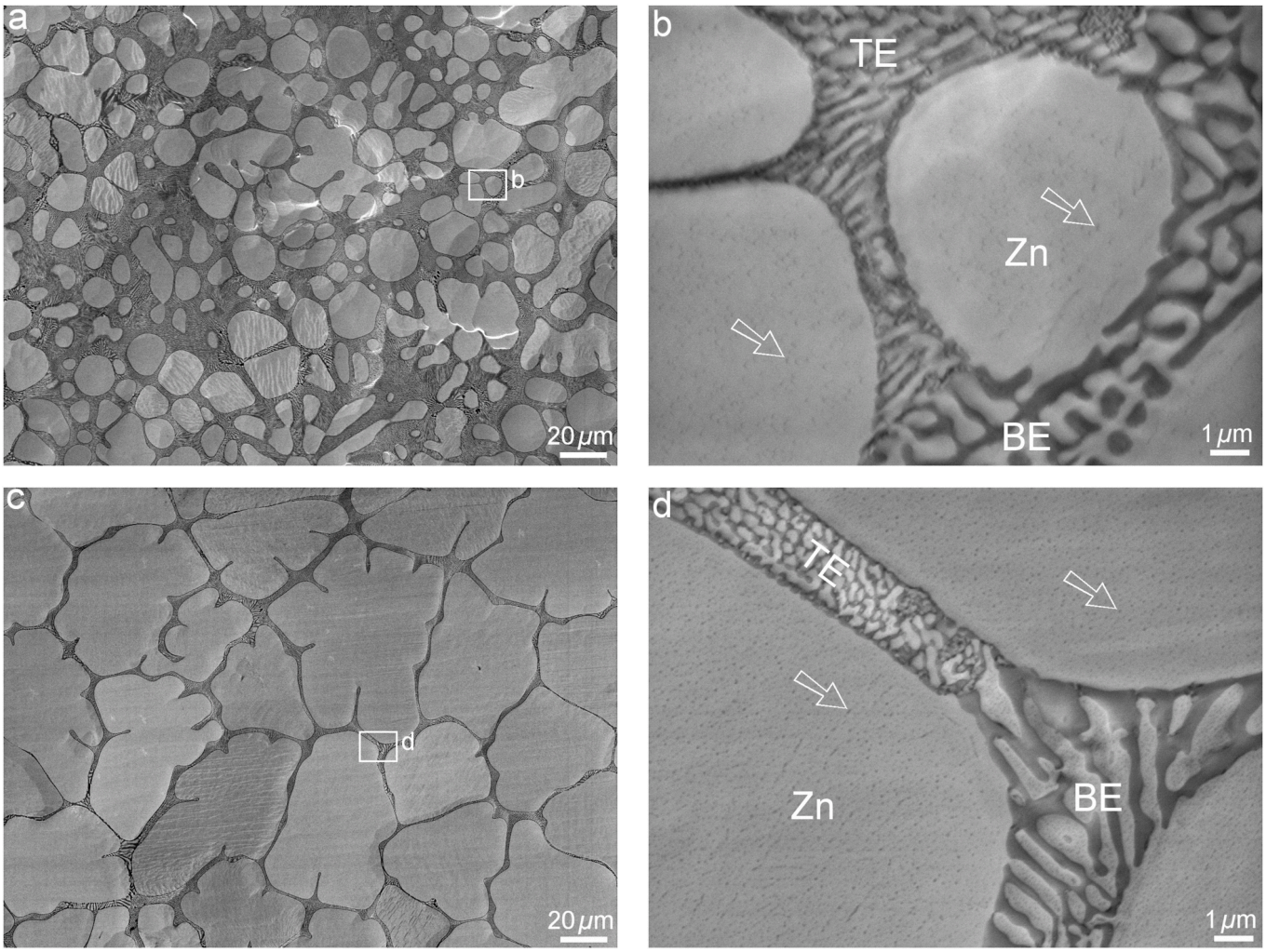

Fig. 2. SEM micrographs of the microstructures of (a) Fine grained ZC1, (b) a magnified region in ZC1 revealing primary Zn grains, fine ternary eutectic (TE) and coarse binary eutectic (BE), (c) Coarse grained ZC2 and (d) a magnified region in ZC2. The arrows indicate the precipitates.

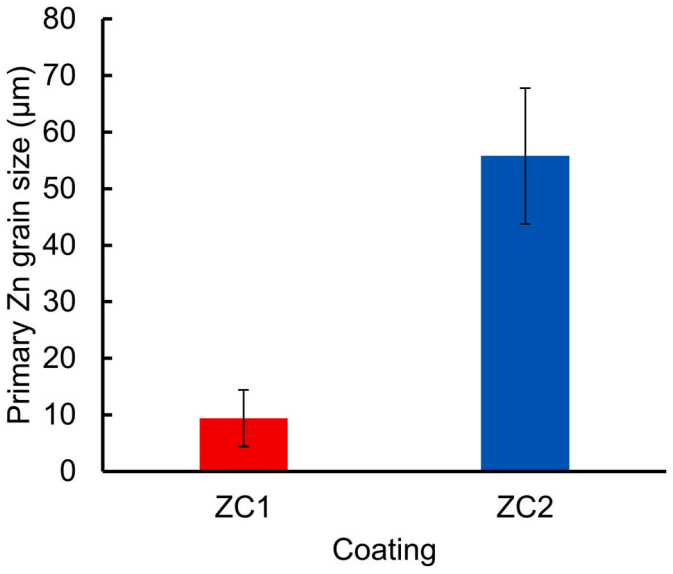

Fig. 3. Comparison of the primary Zn grain sizes in the ZC1 and ZC2 coatings.

formability and cracking of these coatings. In particular, we have previously shown that by fostering a favorable (0001) texture, the cracking resistance of the Zn–Al–Mg coatings can be significantly improved [29]. Here, the large areas selected from the gauge of the ZC1 and ZC2 tensile specimens were subjected to EBSD analysis and the results are depicted in Fig. 4 and Fig. 5. Fig. 4a–c illustrate the image quality (IQ) map, inverse pole figure (IPF) map and the crystallographic texture representation using pole figures (PFs). As it can be observed in Fig. 4a, a homogenous fine grain microstructure of the coating ZC1 is revealed, while the coating ZC2 exhibits uniform and coarse primary zinc grains as Fig. 5a demonstrates. The majority of the microstructural components are detected in red signifying the (0001) orientation tendency for both coatings. As Figs. 4c and 5c illustrate, both of the coatings possess a concentrated and strong (0001) fiber texture. This observation is critical, because in order to be able to compare the deformation response of the coatings, a relatively similar texture is required. Having realized this condition, two areas from the ZC1 and ZC2 are selected (as specified by a rectangle in Fig. 4a and b) and subjected to *in-situ* uniaxial tensile tests as discussed in the next section.

3.3. *In-situ SEM tensile tests*

In-situ SEM tests offer the possibility to track and observe the local generation and evolution of cracks within the microstructure. Accordingly, the coating ZC1 and ZC2 on steel substrates were subjected to *in-situ* tensile tests and the resultant true stress-strain curves are displayed

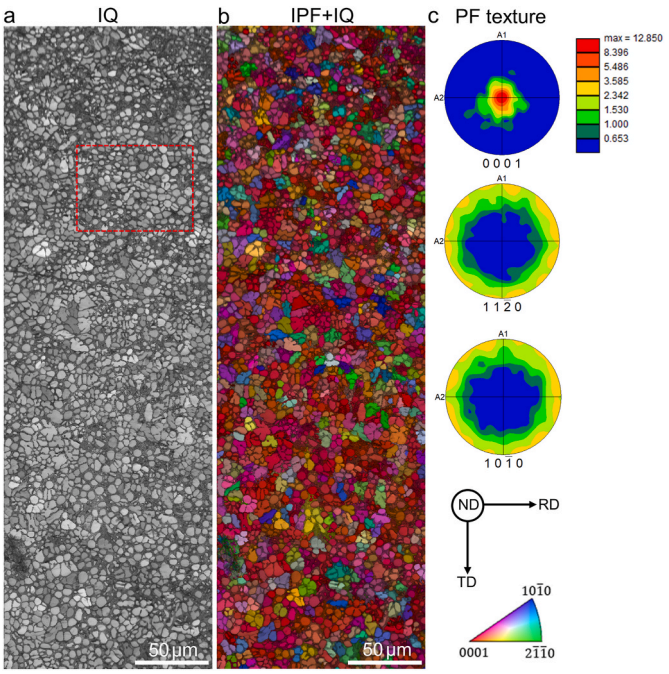

Fig. 4. EBSD analysis results of the ZC1 coating microstructure prior to the tensile deformation, (a) IQ map, (b) IPF + IQ map and (c) crystallographic texture shown by PFs.

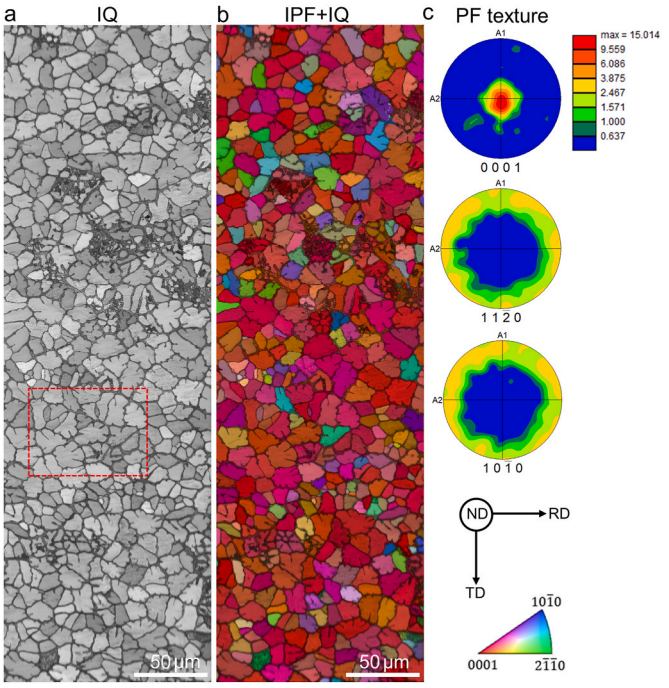

Fig. 5. EBSD analysis results of the ZC2 coating microstructure prior to the tensile deformation, (a) IQ map, (b) IPF + IQ map and (c) crystallographic texture shown by PFs.

in Fig. 6. The corresponding SEM micrographs at each interruption of straining associated with the ZC1 and ZC2 are illustrated in Fig. 7 and Fig. 8, respectively. The true strain values are indicated on the top right of the corresponding SEM images. It should be pointed out that the same field of view is kept for the successive observation and tracked for both of the coatings to make a fair comparison.

As it can be noticed in Figs. 7 and 8, the ZC1 sample begins to show

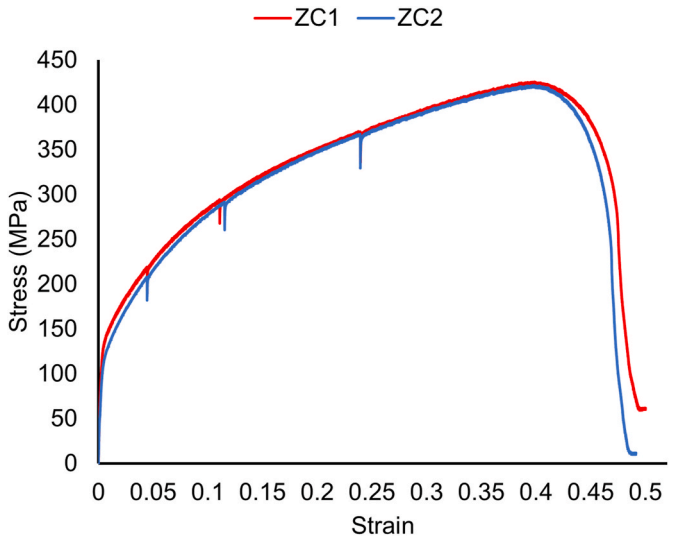

Fig. 6. The true stress-strain curves of the coatings on a same steel substrate attained by performing *in-situ* tensile tests. The small drops in the curves are due to the applied interruptions for SEM characterization of the microstructures at different strain levels.

micro-cracking from early stage of the deformation at true strain of 0.05. Nevertheless, the size of these micro-cracks are found to be less than 3 μm on an average. As the tensile deformation continues to 0.1 strain, the number of the micro-cracks increases sharply as Fig. 7c presents. Most of these cracks are nucleated in the weak and less formable BE platelets, as the mechanism of such cracking is described in our earlier investigations [23]. By approaching the end of the tensile test, these cracks enlarge but remain confined in the eutectic regions. In other words, nearly all of the micro-cracks in the ZC1 are restricted to the eutectic components without propagating into the adjacent primary zinc grains. This fact plays a significant role in the cracking resistance of the coating. In the case of the coating ZC2, one can observe that the initiation of micro-cracking in the binary eutectics occurs at 0.05 true strain as illustrated in Fig. 8b. However, the most significant observation in this stage is the formation of abundant coarse deformation twins as designated by arrows in Fig. 8b. By reaching higher strain values, more cracks are formed in the BE component of the coating. Nevertheless, the major difference here is related to the propagation capability of the cracks. In contrast to the ZC1 with finer grains, the ZC2 exhibiting coarse grains experiences abundant transgranular crack propagations into Zn grains starting from 0.25 true strain. By a close view shown in Fig. 8f, the micro-crack generated in BE, has further propagated through the adjacent Zn grain resulting in a larger crack. It is important to note that this propagating site of the cracking is at the twin boundary within the grain. In particular, some twins which are formed in the Zn grains (see Fig. 8b) serve as a preferential sites for crack propagation. Among those, G1 and G2 are specifically indicated in Fig. 8d. From another point of view, the coarse primary zinc grains surrounded by the eutectic phases carry the majority of the microscopic strain as shown previously [24]. Due to the sharp strain contrast in Zn grains and the surrounding eutectics, large Zn grains in the ZC2 seem to experience a geometrical incompatibility to accommodate the deformation as Fig. 8 indicates. Consequently, more severe in-grain distortions are detectable in the ZC2 in comparison with the ZC1. Such severe distortion can give rise to damage and cracking within the grains. In total, the observed transgranular propagations of the cracks in the coarse Zn grains deteriorate the cracking resistance and formability of these coatings as demonstrated at the end of the tensile test on the ZC2 (see Fig. 8e). It is worth mentioning that both of the coatings, possessing a favorable crystallographic texture, still outperform the coatings with dispersed texture. This topic can be found in detail in our previous publication [29].

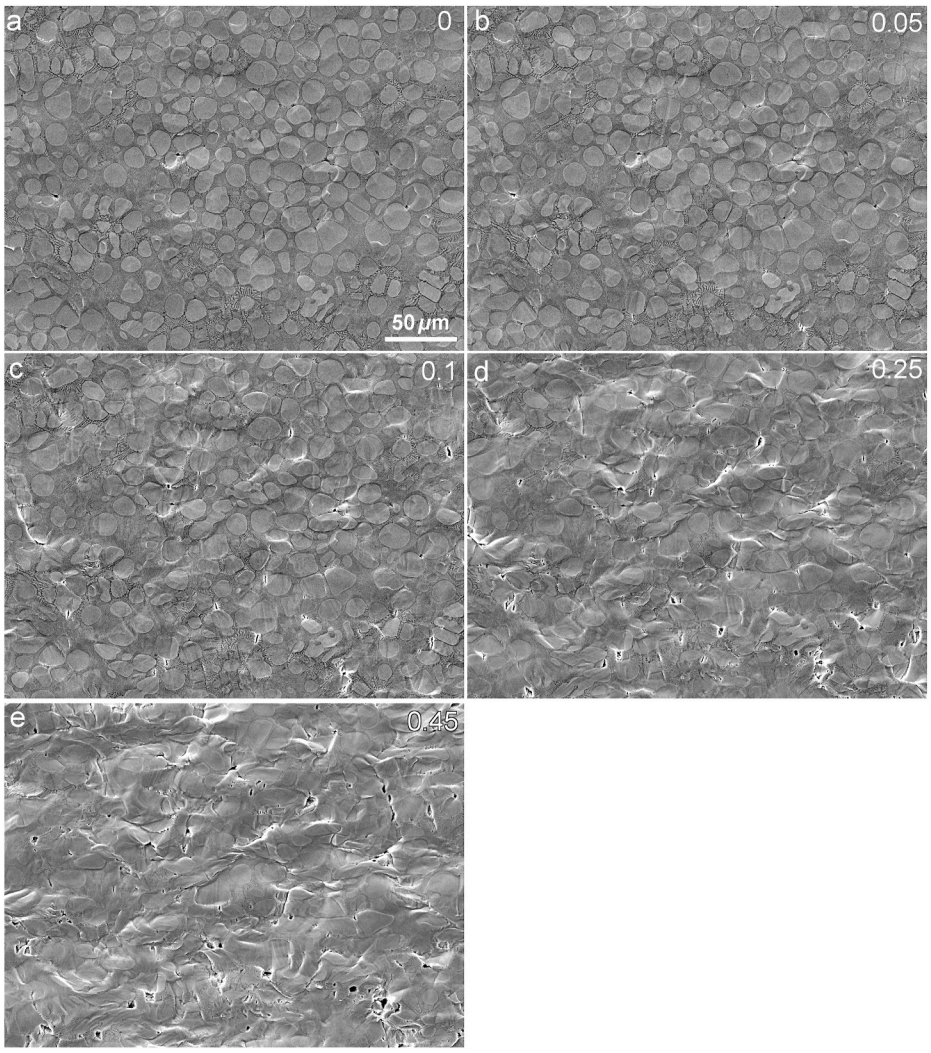

Fig. 7. SEM micrographs of a selected area in the ZC1 coating during *in-situ* tensile test. The true strain value for each interruption is given in the corresponding images at the top-right corner.

3.4. Cracking quantification

In order to compare the cracking tendency of the coatings in a more quantitative way, larger fields of view (FoV) with lower magnification SEM images of the coatings at the end of the tensile tests were captured. Subsequently, the cracking was quantitatively measured by means of image analysis. Fig. 9 shows the large FoV micrographs of the ZC1 and ZC2 coatings. The quantification of the crack area fraction within the coatings is provided in Fig. 10.

Figs. 9 and 10 evidently demonstrate the higher cracking tendency of the ZC2. Fig. 9 confirms the previous observations in Section 3.3, i.e. the cracks in the ZC1 are dominantly created and confined in the eutectic components lacking the possibility to form a large open crack. On the contrary, the ZC2 exhibits coalesced cracks with larger openings. These results imply that the Zn–Al–Mg coatings with large grain sizes are more prone to severe cracking in comparison with the coatings with the fine grains. It should be mentioned that due to the larger fraction of binary eutectic in the coating ZC1 (see Fig. 2), the initiation site density of the cracks is expected to be higher for the ZC1 compared to that of the ZC2. Nevertheless, the transgranular propagations via primary zinc grains are the more detrimental aspect of cracking (specially for corrosion protection), rather than the confined microcracks in the eutectic regions. This transgranular cracking is mostly attributed to the higher probability of twin formation (elaborated in the next section) and the geometrical incompatibilities that occur within the coarse Zn grains of ZC2.

3.5. EBSD analysis after deformation

EBSD analysis can reveal the deformation response of the coatings at the grain level. Earlier in this study it was demonstrated that Zn–Al–Mg coating microstructures with different grain sizes show distinct deformation and cracking behaviors. In this section, it is intended to further investigate the deformation response of the coatings using the EBSD technique. To this purpose, the EBSD analyses were executed on the ZC1 and ZC2 coatings deformed up to 0.1 true strain and the results are displayed in Fig. 11.

As it can be observed in Fig. 11, the crystallographic textures of both coatings have been transformed from the initial state of the texture prior to deformation (see Fig. 5). The fully concentrated sharp (0001) texture is altered to a relatively disperse texture as the pole figures indicate. The dominant change in the texture is attributed to the twin formation. In particular, as Fig. 11 depicts, the ZC2 exhibits substantial higher numbers of twining events per grain compared to the ZC1. The deformation mechanisms of the ZC2 seem to be governed mostly by twinning rather than slip. This is in a good agreement with the findings in *in-situ* SEM tensile tests provided in Section 3.3. As Fig. 11b indicates, the change in the texture is accumulated in certain areas of the pole figures indicated by arrows. To further clarify this and elucidate the grain level

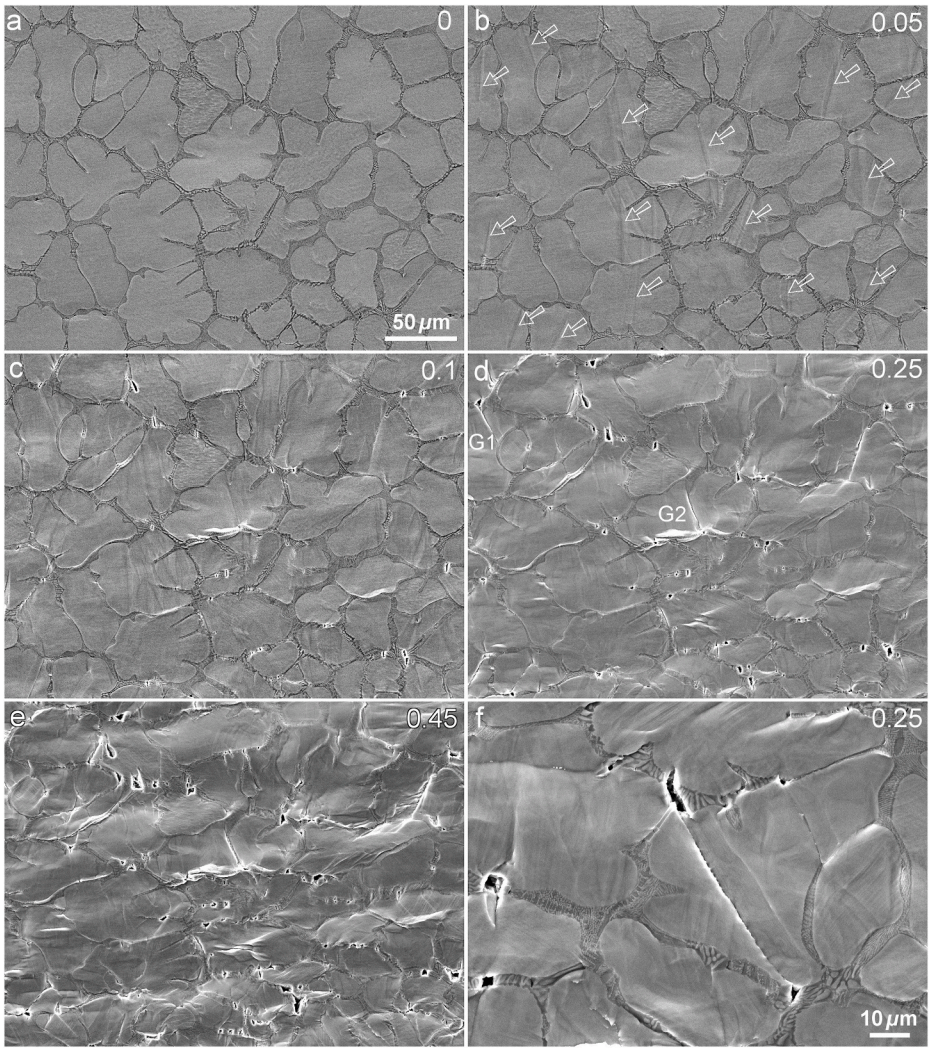

Fig. 8. SEM micrographs of a selected area in the ZC2 coating during *in-situ* tensile test. The true strain value for each interruption is given at the top-right corner of the corresponding image. The arrows indicate the deformation twinning inside the Zn grains. (f) A close view of a propagated crack in another area of the microstructure at 0.25 true strain.

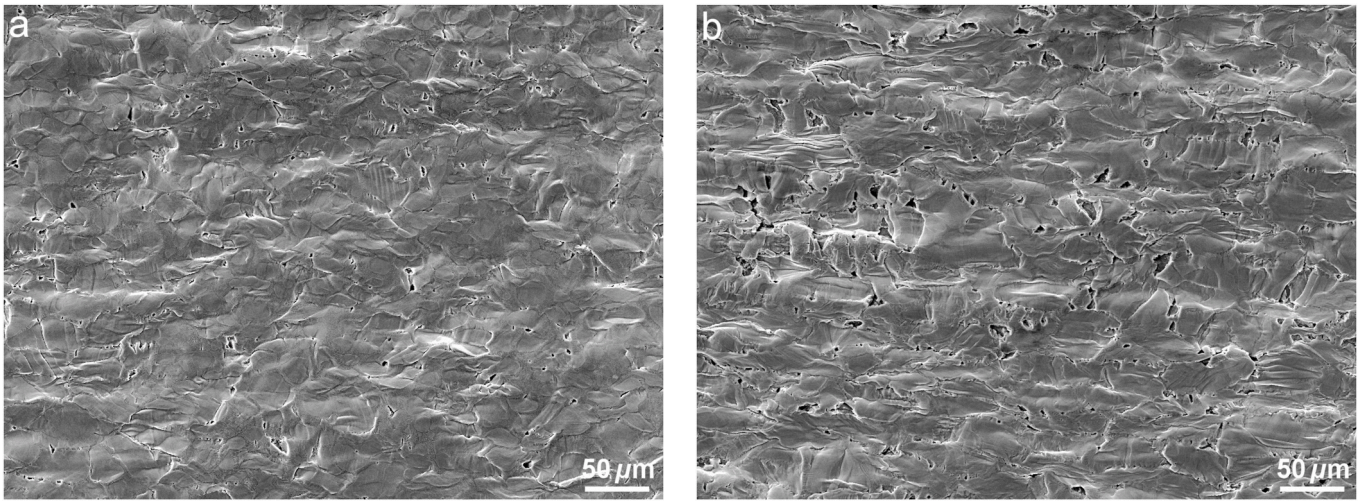

Fig. 9. Comparison between the cracking tendency of the coatings using large field of view SEM images at the end of tensile test (i.e. true strain of 0.45): (a) ZC1 and (b) ZC2.

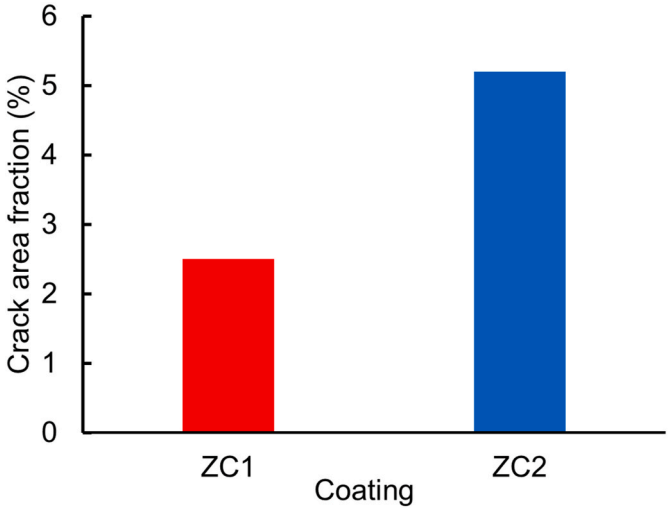

Fig. 10. The quantification of the crack area fraction within the examined coatings.

deformation and damage response of the ZC2 coating, a smaller region is selected (see Fig. 11b) and the results of the meticulous EBSD analysis are provided in Fig. 12. In particular, Fig. 12a depicts the IPF map merged with IQ, Fig. 12b demonstrates the local orientation spread (LOS) map and Fig. 12c shows the misorientation distribution along an arrow drawn on the grain 3 (G3).

As it can be noticed in Fig. 12, most of the grains (e.g. G3 and G5) in the selected region exhibit twins. Yet, a few of the grains are not deformed via twinning (e.g. G4). Fig. 12c implies that the twin formed in G3 exhibits 90° misorientation with the parent grain, approving the tensile (extension) nature of the twin in HCP Zn [37]. This describes the change in the texture demonstrated by PFs in Fig. 11b. Moreover, the LOS map in Fig. 12b gives an interesting description in terms of the deformation for the individual grains of the ZC2 microstructures. As it can be conceived, G3 and G5 possessing twins exhibit a higher LOS value (especially at the twin boundaries) in comparison with G4 without twinning. Higher LOS values are indicative of higher extent of micro damage [23]. Therefore, G3 and G5 are potentially susceptible to damage and cracking due to the coarse twins and higher in-grain LOS values. In contrast, G4 with an unfavorable orientation for twinning leaves no twin behind and results in a less in-grain LOS value. This strongly supports the elucidations for the damage and micro-crack incidents previously observed on twinned grains of the ZC2 shown in Fig. 8. Fig. 13 displays the differences in the deformation of grains in the ZC1 and ZC2 coatings using representative SEM images taken after the tensile test to 0.1 strain. The grains of the refined ZC1 are dominantly deformed through slip as demonstrated by slip traces detected in Fig. 13a; whereas the grains in the coarse-grained ZC2 are mostly undergone twinning as Fig. 13b indicates. This suggests that not only the cracking extent, but also the deformation mechanism in Zn–Al–Mg coatings are grain size dependent.

Zinc and its alloys with inhomogeneous and multiphase structures predominantly show complex deformation behavior. In particular, these complexities add up when it comes to Zn alloy coatings due to their small thickness (usually around 10–15 μm) and difficulties in sample preparation and controlled experimental testing. It has been the subject of various studies to increase the strength and ductility of pure zinc and zinc alloy materials by nurturing grain refinement in the microstructure. In the Zn–Al–Mg coatings family, this study is the first attempt to tackle the deformation and cracking performance as a function of grain size. As it was shown earlier in this research, the grain refinement considerably affects the plasticity and cracking resistance of these coatings. These pronounced behaviors can be explained by the following concurrent phenomena and mechanisms, where the first two items mainly concern strengthening aspect:

(1) Grain boundary strengthening (σ) is modeled by the well-known Hall-Petch equation as $\sigma = \sigma_0 + kd^{-1/2}$, where σ_0, k and d denote the friction stress, a constant and material grain size, respectively [38]. According to this expression, the coating ZC1 (d = 9 μm) triggers higher grain boundary strengthening compared to the coating ZC2 (d = 56 μm). This signifies that the larger grain boundary area per unit volume impedes dislocation motion (and also causes more dislocation generation, accumulation and annihilation at the boundaries) giving rise to the strength of the

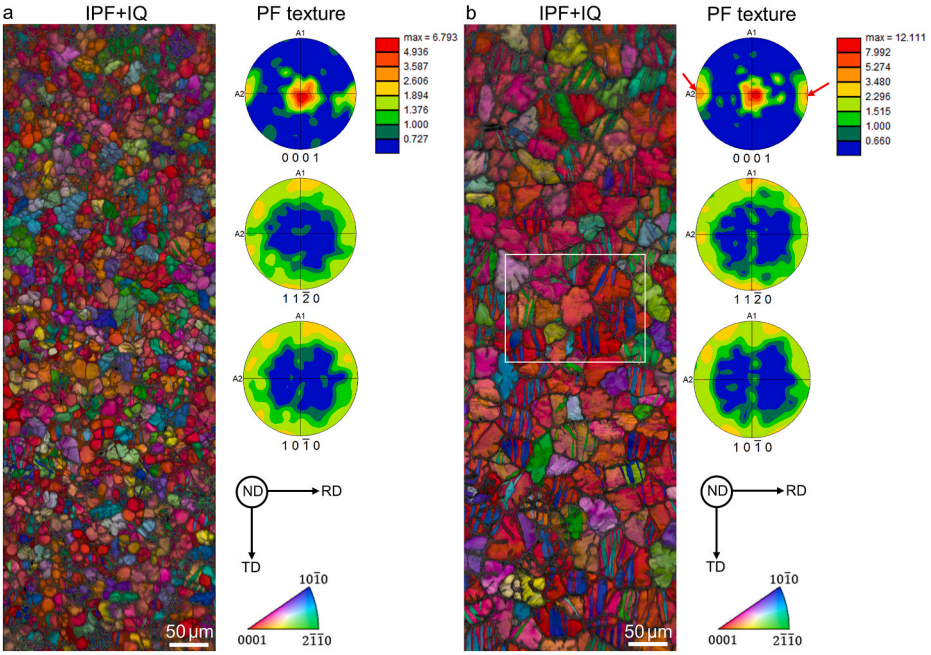

Fig. 11. EBSD results on the coatings deformed up to 0.1 true strain, (a) ZC1 and (b) ZC2.

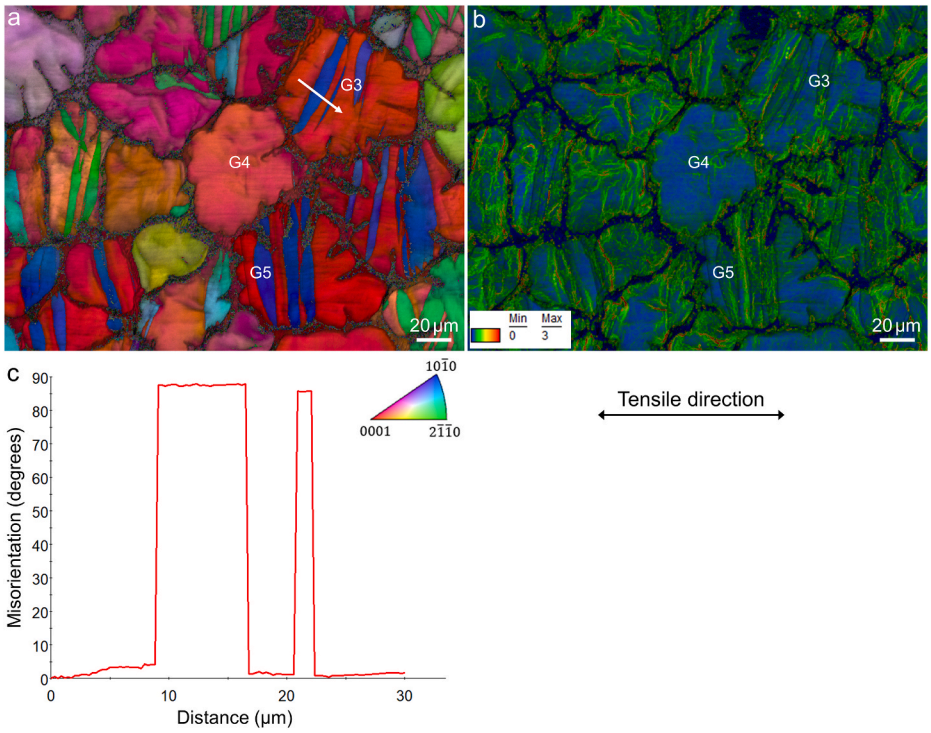

Fig. 12. (a) IPF map of a selected region within the ZC2 microstructure deformed up to 0.1 true strain, (b) the LOS map, (c) misorientation distribution along the arrow designated in (a).

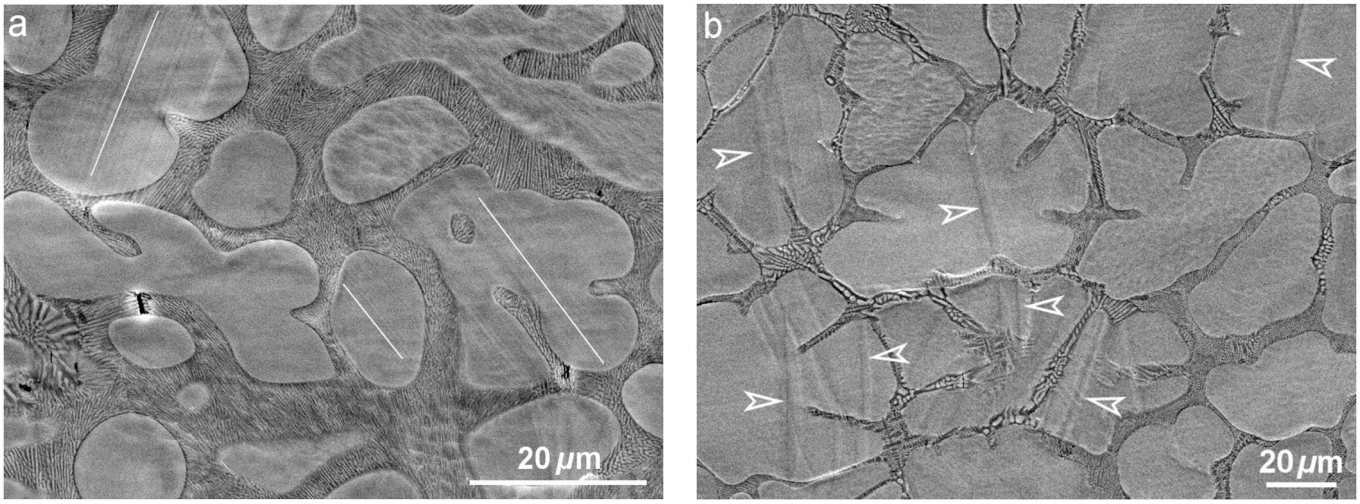

Fig. 13. Representative SEM micrographs showing the microstructure of the coatings deformed until a true strain of 0.1 during tensile test: (a) ZC1 and (b) ZC2.

coating. In addition, grain boundaries impede the micro-cracks formed in the BE and prevent them from propagating.

(2) The eutectic components of the coating, in particular the fiber-like ternary eutectic, play an import morphological role in the strengthening and plasticity of the coating. Due to the finer structures of eutectic constituents comprising of Mg–Zn intermetallic compounds, they notably contribute to the total strengthening of the coating [24]. Since the coating ZC1 with finer primary Zn grain size possesses a higher fraction of the ternary eutectic within its microstructure compared to that of the ZC2, one expect the total strengthening of the ZC1 increases further via this contribution.

(3) The differences in the primary Zn grain sizes in the examined coatings suggest another (more) significant aspect. The ZC1 possesses Zn grains with sizes less than the thickness of the coating (i.e. 15 μm), whereas the ZC2 exhibits a grain size much larger (almost 5 times) than the coating thickness. Consequently, it is more convenient for the ZC1 to accommodate the imposed plastic deformation. In contrast, the microstructure of the ZC2 will undergo stress concentrations especially along the thickness leading to the in-grain distortion and damage.

(4) The contrast in the mechanical properties between the primary zinc grains and eutectic components generates a stress/strain gradient both at the interphases and along the thickness of the coatings [24,26]. Such gradient seems to contribute to the in-grain geometrical distortion/incompatibilities of the primary zinc grains within the ZC2, making the ZC2 much harder to deform without damage compared to the ZC1.

(5) Not only the strengthening mechanism can be boosted through grain refinement, but also the ductility can be increased. As it has been manifested by various studies on HCP metals [34], grain refinement prompts the activation of non-basal slip systems and consequently enhances the ductility of the material. Grain refinement can also shorten the dislocation slip trajectory which leads to easier grain boundary movement and grain rotation during the deformation [39].

(6) As it was elucidated in Sections 3.4 and 3.5, by increasing the grain size, the cracking tendency of the coating ZC2 increases chiefly due to the prevalent tensile twins. Whereas smaller grain sizes tend to increase the slip activation probability (Fig. 13a). Deformation twinning is shown to be an abundant mode of plastic deformation in HCP metals, specifically when the slip mechanism are retarded [40]. In contrast to slip mode deformation, twinning creates three dimensional sub-crystalline domains which consequently induce internal stress fields within the grains. This is typically followed by a large shear between the twin boundary and the parent grain [41,42]. Moreover, deformation twinning is found to be more activated at the free surfaces (like those of the coatings) compared to the bulk material when subjected to plastic deformation [42]. Such coarse twin lamellae generated in the coarse-grained ZC2 coating, trigger high internal stress fields and subsequent damage within the Zn grains. This was confirmed in Fig. 12 by higher in-grain LOS values (e.g. for twinned G3 and G5) in contrast to low LOS value in the twin-free grains (e.g. G4). The above explanations elucidate the main contributing reasons of the damage and transgranular crack propagations in primary zinc grains which can further deteriorate other functionalities of the coatings including corrosion resistance. Therefore, promoting the slip activity by refining the microstructure of the Zn–Al–Mg coatings can notably boost the cracking resistance and formability.

To put the present results in a broader picture on the plastic deformation and cracking in Mg-alloyed zinc coatings, it is worthwhile to summarize the state of the art knowledge generated on this topic. Mg-alloyed zinc coatings, including the Zn–Al–Mg coating family, perform poorly under different loading conditions. There have been a few valuable attempts to understand the cracking in these coating systems which are of significant practical applications [3,27,28]. We have comprehensively tackled the deformation and cracking behaviors of these coating in our previous studies with different key points of attention and approaches. By understanding the cause and mechanism of cracking and generating a quantitative/predictive methodology [23], the microstructure of the Zn–Al–Mg coatings was tailored by eliminating the BE component [24]. This led to substantial improvement in cracking resistance through dislocation driven strengthening and plasticity. We consequently elucidated the influence of the steel substrates on cracking and formability of these coatings [26]. The cracking resistance of the Zn–Al–Mg coatings were improved by utilizing a ductile steel substrate without discontinuous yielding. The crystallographic texture control further enabled to prevent the cracking and inhibit the propagation of the cracks within the coating microstructures [29]. Ultimately this study uncovers another significant factor (i.e. grain refinement) for the crack suppression and enhancement of formability properties in Zn–Al–Mg coatings. The framework established above provides a foundation to design and optimize the structure-properties relationship for the next generation highly formable Zn–Al–Mg coatings by fostering synergic solutions (i.e. controlling phases, texture, grain sizes and coating-substrate combination).

4. Conclusions

In this paper, we have explored the deformation characteristics and cracking resistance of Zn–Al–Mg coatings on steel substrate as a function of the grain sizes. Microstructural level investigations imply the significance of the grain refinement in the deformation behavior of multi-phase zinc alloy coatings. The cracking extent is quantified for two coatings with distinctly different grain sizes when subjected to *in-situ* SEM uniaxial tensile tests. The most notable conclusions of this work are as follows:

- Zn–Al–Mg coating with fine primary Zn grain microstructure exhibits higher cracking resistance and formability capacity in comparison with the coating possessing coarse Zn grains.
- Both deformation mechanisms and cracking behavior are found be to grain size dependent in Zn–Al–Mg coatings.
- The plastic deformation in fine grain coating is predominantly governed by slip mechanisms, whereas it is controlled by prevalent deformation twinning for the coarse grain coating.
- Deformation twinning induces in-grain distortions/damage and triggers intergranular cracking within the coarse Zn grains.
- By stimulating grain refinement and decreasing the possibility of coarse twinning incidents, it is possible to enhance the cracking resistance and formability of Zn–Al–Mg coatings.

Funding

This research was funded under project number S22.3.15576/15440 by the Partnership Program of the Materials innovation institute M2i (www.m2i.nl) and the Technology Foundation TTW (www.stw.nl), which is part of the Netherlands Organization for Scientific Research (www.nwo.nl).

CRediT authorship contribution statement

Masoud Ahmadi: Conceptualization, Methodology, Investigation, Data curation, Formal analysis, Visualization, Validation, Writing – original draft. **Bekir Salgın:** Resources, Writing – review & editing. **Bart J. Kooi:** Formal analysis, Writing – review & editing, Supervision. **Yutao Pei:** Conceptualization, Formal analysis, Funding acquisition, Writing – review & editing, Supervision.

Declaration of competing interest

The authors declare that they have no known competing financial interests or personal relationships that could have appeared to influence the work reported in this paper.

References

[1] P.K. Rai, D. Rout, D.S. Kumar, S. Sharma, G. Balachandran, Effect of magnesium on corrosion behavior of hot-dip Zn-Al-Mg coating, J. Mater. Eng. Perform. 30 (2021) 4138–4147.
[2] T. Prosek, D. Persson, J. Stoulil, D. Thierry, Composition of corrosion products formed on Zn–Mg, Zn–Al and Zn–Al–Mg coatings in model atmospheric conditions, Corrosion Sci. 86 (2014) 231–238.
[3] E. De Bruycker, Z. Zermout, B.C. De Cooman, Zn-Al-Mg coatings: thermodynamic analysis and microstructure related properties, Mater. Sci. Forum 539–543 (2007) 1276–1281. 10.4028/www.scientific.net/MSF.539-543.1276.
[4] T. Truglas, J. Duchoslav, C. Riener, M. Arndt, C. Commenda, D. Stifter, G. Angeli, H. Groiss, Correlative characterization of Zn-Al-Mg coatings by electron microscopy and FIB tomography, Mater. Char. (2020) 110407.
[5] N. LeBozec, D. Thierry, D. Persson, C.K. Riener, G. Luckeneder, Influence of microstructure of zinc-aluminium-magnesium alloy coated steel on the corrosion behavior in outdoor marine atmosphere, Surf. Coating. Technol. 374 (2019) 897–909.
[6] Y. Meng, G. Jiang, X. Ju, J. Hao, TEM study on the microstructure of the Zn-Al-Mg alloy, Mater. Char. 129 (2017) 336–343, https://doi.org/10.1016/j.matchar.2017.05.011.
[7] C. Commenda, J. Pühringer, Microstructural characterization and quantification of Zn-Al-Mg surface coatings, Mater. Char. 61 (2010) 943–951, https://doi.org/10.1016/j.matchar.2010.06.008.
[8] C. Yao, H. Lv, T. Zhu, W. Zheng, X. Yuan, W. Gao, Effect of Mg content on microstructure and corrosion behavior of hot dipped Zn–Al–Mg coatings, J. Alloys Compd. 670 (2016) 239–248, https://doi.org/10.1016/j.jallcom.2016.02.026.

[9] S. Li, B. Gao, S. Yin, G. Tu, G. Zhu, S. Sun, X. Zhu, The effects of RE and Si on the microstructure and corrosion resistance of Zn-6Al-3Mg hot dip coating, Appl. Surf. Sci. 357 (2015), https://doi.org/10.1016/j.apsusc.2015.09.172, 2004–2012.

[10] S. Zhou, C. Shen, S. Han, Q. Tao, Z. Chen, Effects of Ce and in on microstructure and corrosion properties of Zn-9Al-2.5Mg alloy, Mater. Res. Express 6 (2019) 2–11, https://doi.org/10.1088/2053-1591/ab120f.

[11] M. Zhang, G. Zhou, H. Sun, X. Teng, Z. Zhao, Effect of Ti and Zr elements with equal mass ratio on microstructure and corrosion resistance of Zn-11Al-3Mg alloy, Mater. Corros. (2020), https://doi.org/10.1002/maco.202011723.

[12] L. Hai Tat, H.R. Bakhsheshi-Rad, E. Hamzah, M.H. Cho, A. Mostafa, S. Farahany, Microstructure, phase evolution and corrosion behaviour of the Zn–Al–Mg–Sb alloy coating on steel, Mater. Sci. Technol. 36 (2020) 353–366.

[13] Z. Gabalcová, P. Gogola, M. Kusý, H. Suchánek, The effect of Sn addition on Zn-Al-Mg alloy; Part II: corrosion behaviour, Materials (Basel) 14 (2021) 5290.

[14] R. Parisot, S. Forest, A. Pineau, F. Grillon, X. Demonet, J.-M. Mataigne, Deformation and damage mechanisms of zinc coatings on hot-dip galvanized steel sheets: Part II. Damage modes, Metall. Mater. Trans. A. 35 (2004) 813–823.

[15] J. He, J. Lian, A. Aretz, N. Vajragupta, U. Hangen, F. Goodwin, S. Münstermann, Fracture properties of zinc coating layers in a galvannealed steel and an electrolytically galvanized steel, Mater. Sci. Eng. A. 732 (2018) 320–325, https://doi.org/10.1016/j.msea.2018.05.084.

[16] L. Cauvin, B. Raghavan, S. Bouvier, X. Wang, F. Meraghni, Multi-scale investigation of highly anisotropic zinc alloys using crystal plasticity and inverse analysis, Mater. Sci. Eng. A. 729 (2018) 106–118.

[17] J. Legendre, R. Créac'Hcadec, A. Tanguy, S. Hallais, J.-H. Schmitt, E. Héripré, F. Gilbert, D. Jacquet, J.M. Mataigne, A unique combination of in-situ and multi-scale methodologies to analyze damage mechanisms of temper rolled zinc coating, Mater. Sci. Eng. A. 763 (2019) 138156.

[18] J.H. Liu, C.X. Huang, S.D. Wu, Z.F. Zhang, Tensile deformation and fracture behaviors of high purity polycrystalline zinc, Mater. Sci. Eng. A. 490 (2008) 117–125, https://doi.org/10.1016/j.msea.2008.01.004.

[19] G. Dirras, J. Gubicza, H. Couque, A. Ouarem, P. Jenei, Mechanical behaviour and underlying deformation mechanisms in coarse- and ultrafine-grained Zn over a wide range of strain rates, Mater. Sci. Eng. A. 564 (2013) 273–283, https://doi.org/10.1016/j.msea.2012.12.010.

[20] G.-M. Song, W.G. Sloof, Characterization of the failure behavior of zinc coating on dual phase steel under tensile deformation, Mater. Sci. Eng. A. 528 (2011) 6432–6437.

[21] W. Bednarczyk, M. Wątroba, J. Kawałko, P. Bała, Can zinc alloys be strengthened by grain refinement? A critical evaluation of the processing of low-alloyed binary zinc alloys using ECAP, Mater. Sci. Eng. A. 748 (2019) 357–366, https://doi.org/10.1016/j.msea.2019.01.117.

[22] C.P. Camurri, R.G. Benavente, I.S. Roa, C.C. Carrasco, Deformation and fatigue behavior of hot dip galvanized coatings, Mater. Char. 55 (2005) 203–210, https://doi.org/10.1016/j.matchar.2005.05.005.

[23] M. Ahmadi, B. Salgın, B.J. Kooi, Y. Pei, Genesis and mechanism of microstructural scale deformation and cracking in ZnAlMg coatings, Mater. Des. 186 (2020) 108364, https://doi.org/10.1016/j.matdes.2019.108364.

[24] M. Ahmadi, B. Salgın, M. Ahmadi, B.J. Kooi, Y. Pei, Unraveling dislocation mediated plasticity and strengthening in crack-resistant ZnAlMg coatings, Int. J. Plast. 144 (2021) 103041, https://doi.org/10.1016/j.ijplas.2021.103041.

[25] G. Vincent, N. Bonasso, J.S. Lecomte, B. Colinet, B. Gay, C. Esling, The relationship between the fracture toughness and grain boundary characteristics in hot-dip galvanized zinc coatings, J. Mater. Sci. 41 (2006) 5966–5975, https://doi.org/10.1007/s10853-006-0274-6.

[26] M. Ahmadi, B. Salgın, B.J. Kooi, Y. Pei, Cracking behavior and formability of Zn-Al-Mg coatings: understanding the influence of steel substrates, Mater. Des. 212 (2021) 110215, https://doi.org/10.1016/J.MATDES.2021.110215.

[27] H. Zunko, A. Hackl, H. Antrekowitsch, R. Ebner, R. Brisberger, F. Priewasser, C. K. Riener, Analyse des Umformverhaltens von Zn-Al-Mg-Beschichtungen, BHM Berg- Hüttenmännische Monatsh. 154 (2009) 334–341, https://doi.org/10.1007/s00501-009-0482-x.

[28] Y.B. Park, I.G. Kim, S.G. Kim, W.T. Kim, T.C. Kim, M.S. Oh, J.S. Kim, Orientation dependence of cracking in hot-dip Zn-Al-Mg alloy coatings on a sheet steel, Metall. Mater. Trans. A Phys. Metall. Mater. Sci. 48 (2017) 1013–1020, https://doi.org/10.1007/s11661-016-3947-z.

[29] M. Ahmadi, B. Salgın, B.J. Kooi, Y. Pei, Outstanding cracking resistance in Mg-alloyed zinc coatings achieved via crystallographic texture control, Scripta Mater. 210 (2022), https://doi.org/10.1016/j.scriptamat.2021.114453.

[30] M. Safaeirad, M.R. Toroghinejad, F. Ashrafizadeh, Effect of microstructure and texture on formability and mechanical properties of hot-dip galvanized steel sheets, J. Mater. Process. Technol. 196 (2008) 205–212, https://doi.org/10.1016/j.jmatprotec.2007.05.035.

[31] C.M. Wichern, B.C. De Cooman, C.J. Van Tyne, Surface roughness changes on a hot-dipped galvanized sheet steel during deformation at low strain levels, Acta Mater 52 (2004) 1211–1222, https://doi.org/10.1016/j.actamat.2003.11.005.

[32] C. Wang, D. Yu, Z. Niu, W. Zhou, G. Chen, Z. Li, X. Fu, The role of pyramidal <c + a> dislocations in the grain refinement mechanism in Ti-6Al-4V alloy processed by severe plastic deformation, Acta Mater 200 (2020) 101–115, https://doi.org/10.1016/j.actamat.2020.08.076.

[33] H. Fan, S. Aubry, A. Arsenlis, J.A. El-Awady, Grain size effects on dislocation and twinning mediated plasticity in magnesium, Scripta Mater. 112 (2016) 50–53, https://doi.org/10.1016/j.scriptamat.2015.09.008.

[34] K. Wei, R. Hu, D. Yin, L. Xiao, S. Pang, Y. Cao, H. Zhou, Y. Zhao, Y. Zhu, Grain size effect on tensile properties and slip systems of pure magnesium, Acta Mater 206 (2021) 116604, https://doi.org/10.1016/j.actamat.2020.116604.

[35] A. Jarzębska, M. Bieda, J. Kawałko, Ł. Rogal, P. Koprowski, K. Sztwiertnia, W. Pachla, M. Kulczyk, A new approach to plastic deformation of biodegradable zinc alloy with magnesium and its effect on microstructure and mechanical properties, Mater. Lett. 211 (2018) 58–61, https://doi.org/10.1016/j.matlet.2017.09.090.

[36] N. Wint, N. Cooze, J.R. Searle, J.H. Sullivan, G. Williams, H.N. McMurray, G. Luckeneder, C. Riener, The effect of microstructural refinement on the localized corrosion of model Zn-Al-Mg alloy coatings on steel, J. Electrochem. Soc. 166 (2019) C3147.

[37] L. Tan, X. Zhang, T. Xia, Q. Sun, G. Huang, R. Xin, Q. Liu, $\{10\bar{1}2\}-\{10\bar{1}2\}$ double tensile twinning in a Mg-3Al-1Zn alloy sheet during cyclic deformation, Mater. Sci. Eng. A. 711 (2018) 205–211, https://doi.org/10.1016/j.msea.2017.11.021.

[38] G. Dirras, A. Ouarem, H. Couque, J. Gubicza, P. Szommer, O. Brinza, Microstructure and nanohardness distribution in a polycrystalline Zn deformed by high strain rate impact, Mater. Char. 62 (2011) 480–487.

[39] Z. Zhang, J. Zhang, J. Wang, Z. Li, J. Xie, S. Liu, K. Guan, R. Wu, Toward the development of Mg alloys with simultaneously improved strength and ductility by refining grain size via the deformation process, Int. J. Miner. Metall. Mater. 28 (2021) 30–45.

[40] M.H. Yoo, Slip, twinning, and fracture in hexagonal close-packed metals, Metall. Trans. A 12 (1981) 409–418.

[41] M. Knezevic, M.R. Daymond, I.J. Beyerlein, Modeling discrete twin lamellae in a microstructural framework, Scripta Mater. 121 (2016) 84–88, https://doi.org/10.1016/j.scriptamat.2016.04.026.

[42] B. Leu, M. Arul Kumar, I.J. Beyerlein, The effects of free surfaces on deformation twinning in HCP metals, Materialia 17 (2021) 101124, https://doi.org/10.1016/j.mtla.2021.101124.